



Sources and meteorological factors that control seasonal variation of $\delta^{34}\text{S}$ values in rainwater

Hong-Wei Xiao ^{a,*}, Hua-Yun Xiao ^{b,*}, Ai-Min Long ^a, Yan-Li Wang ^c, Cong-Qiang Liu ^b

^a State Key Laboratory of Tropical Oceanography, South China Sea Institute of Oceanography, Chinese Academy of Sciences, Guangzhou 510301, China

^b State Key Laboratory of Environment Geochemistry, Institute of Geochemistry, Chinese Academy of Science, Guiyang 550002, China

^c Chinese Research Academy of Environmental Sciences, Beijing 100012, China

ARTICLE INFO

Article history:

Received 28 January 2014

Received in revised form 3 June 2014

Accepted 4 June 2014

Available online 14 June 2014

Keywords:

$\delta^{34}\text{S}$

Sources

Concentration-weighted trajectory

Temperature

Washout

Oxidation pathways

ABSTRACT

Sulfate concentrations and sulfur isotopic compositions were measured in rainwater in Guiyang city in Southwest China between October 2008 and September 2009 to identify sulfur sources and their impacts on sulfur isotopic composition. The $\delta^{34}\text{S}$ values of 1235 samples collected during this period ranged from -12.0 to $+9.4\%$, with a volume-weighted mean of $-2.8 \pm 9.8\%$, suggesting that rainwater sulfate in Guiyang was mainly derived from SO_2 produced during coal combustion. The $\delta^{34}\text{S}$ values of rainwater sulfate increased from 1987 to 2009, with an increment of about $+0.16\%$ per year, reflecting a gradual reduction in ^{34}S -depleted SO_2 emitted during coal combustion. Seasonal variations in $\delta^{34}\text{S}$ values were pronounced, with higher values in winter than in summer. Long-distance transport of SO_2 from coal burned in northern cities (which was higher than the component from southern cities), and more importantly, the aqueous oxidation of SO_2 during transport affected the seasonal variation of rainwater $\delta^{34}\text{S}$ values in Guiyang. Temperature-dependent aqueous oxidation of SO_2 suggested that lower rainwater $\delta^{34}\text{S}$ coincides with higher temperature.

© 2014 Elsevier B.V. All rights reserved.

1. Introduction

The global sulfur cycle has caused widespread concern among international environmental scientists, because it affects global atmospheric pollution, acid deposition, and climate (Kellogg et al., 1972; Andreae et al., 2005). Major inputs of anthropogenic SO_2 into the atmosphere occur in heavily industrialized areas, and are mainly due to the combustion of oils or coals (Kellogg et al., 1972; Li et al., 1999; Mukai et al., 2001; Szykiewicz et al., 2008). Other minor sulfur sources for rainwater sulfate (SO_4^{2-}) include sea spray and biogenic emissions (Rees et al., 1978; Pan et al., 2008; Zhang et al., 2010). In coastal regions, biogenic H_2S and dimethylsulfide (DMS) are both important atmospheric sulfur sources and their emission concentration ratio is about 1:5 (Andreae, 1990).

Rainwater is the main removal mechanism for sulfate (SO_4^{2-}) in the atmosphere (Wadleigh et al., 1996; Xu and Carmichael, 1999; Xiao et al., 2013; Xiao and Liu, 2004), accounting for $>90\%$ of its removal (data from Xiao and Liu, 2004; Xiao et al., 2013). SO_4^{2-} is incorporated into rainwater by in-cloud scavenging (including rainout, nucleation of cloud particles, and formation of SO_4^{2-} from absorbed SO_2 ; Scott and Hobbs, 1967; Scott, 1978) and below cloud scavenging (washout). Generally, in urban areas, formation of SO_4^{2-} from anthropogenic SO_2 is the largest contributor (Wadleigh et al., 1996).

Studies have been carried out all over the world on the sulfur cycle within the atmosphere, using sulfur isotope as a tracer (Saltzman et al., 1983; Mcardel and Liss, 1995; Xiao and Liu, 2002; Xiao et al., 2011). Moreover, sulfur isotopic signatures give us a better understanding of mixing processes, transport, removal, and oxidation pathways in this cycle (Novák et al., 2000, 2001; Xiao and Liu, 2002; Xiao et al., 2009). Both SO_2 and SO_4^{2-} have long residence times in the atmosphere, of about 1 to 2 days and 2 to 4 days, respectively

* Corresponding authors. Tel.: +86 20 89101332.

E-mail addresses: xiaohw@scsio.ac.cn (H.-W. Xiao), xiaohuayun@vip.skleg.cn (H.-Y. Xiao).

(Berglen et al., 2004; Rotsayn and Lohmann, 2002; Tsai et al., 2010). Hence, sulfur-containing aerosols can be transported thousands of kilometers downwind from their origin (Karnieli et al., 2009). Sulfur is one of the major components of fine aerosol particles over continental areas (Quinn and Coffman, 1998). SO_2 sources have different sulfur isotope compositions, depending on the isotopic values of their source materials (Mukai et al., 2001). The $\delta^{34}\text{S}$ of sea salt sulfate is +21.0‰, $\delta^{34}\text{S}$ of H_2S is –30‰ to –6‰, $\delta^{34}\text{S}$ of DMS is +19.8% (Rees et al., 1978; Krouse and Van Everdingen, 1984; Calhoun and Bates, 1989; Herut et al., 1995; Amrani et al., 2013), while the $\delta^{34}\text{S}$ of anthropogenic SO_2 has a wide range of values (Calhoun and Bates, 1989; Hong et al., 1994). Thus, the $\delta^{34}\text{S}$ in rainwater is mainly controlled by the composition of its sulfur source (Wadleigh et al., 1996).

The rapid growth of both industrial and agricultural production during the last two decades has resulted in serious acidic rain problems in many cities in China, e.g., Guiyang (Xiao et al., 2013). Anthropogenic SO_2 emissions are very different among Chinese provinces, with higher emissions in north and east China, and lower emissions in south and west China (Fig. 1), related to different economic development in these regions. Atmospheric SO_2 in China is mainly derived from coal combustion (Galloway et al., 1987; Liu et al., 2011). Despite a decreasing trend of SO_2 emissions

(Fig. 2), it is still the most important factor contributing to acidic rainwater in Guiyang (Xiao et al., 2013). Hence, sulfur isotopic composition has been studied within the city to constrain the sources of sulfur in the atmosphere. Hong et al. (1994) found that summer rainwater $\delta^{34}\text{S}$ values were the lowest, reflecting the presence of biogenic sulfur in the atmosphere. Xiao and Liu (2002) suggested that negative $\delta^{34}\text{S}$ values of light rainfalls were associated with local sources, while sulfur in heavy rainfalls was derived from maritime sources and had positive $\delta^{34}\text{S}$ values in Guiyang. Values of $\delta^{34}\text{S}$ in atmospheric particulate matter in Guiyang were measured by Liu et al. (1996a, 1996b); they reported that coarse particles derived from soil averaged –2.2‰; while fine particles derived mainly from coal combustion averaged –2.3‰.

However, the mechanisms underlying the seasonal variation in rainwater $\delta^{34}\text{S}$ in this city are still unclear. Guiyang has a high rainfall (about 1200 mm per year), so it is an ideal location to study sulfur isotope fractionation in rainwater. In this study, we investigated SO_4^{2-} concentrations and $\delta^{34}\text{S}$ values in rainwater in Guiyang from October 2008 to September 2009. Since acid rain is a common occurrence in this city, we investigated: (1) sources of atmospheric sulfur, and (2) how and why atmospheric sulfur isotopic composition changes with time.

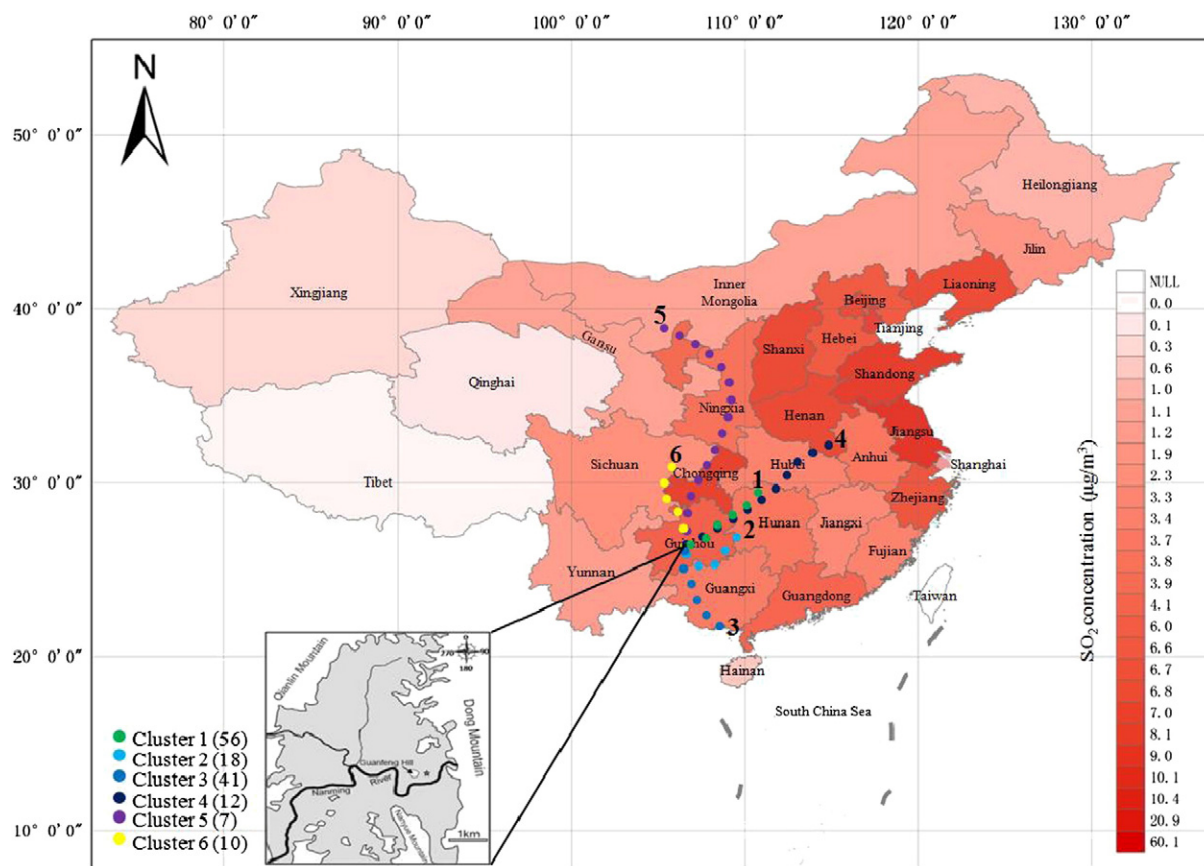


Fig. 1. Map showing sampling location in Guiyang, anthropogenic SO_2 emission ($\mu\text{g}/\text{m}^3$) in different provinces in China in 2009 and three-day mean trajectory clusters ended at Guiyang with polluted trajectory number (the number of different color dotted lines means the number of trajectory from this cluster; the data of SO_2 emission from China Environment Statistical Yearbook, 2010).

2. Experiment

2.1. Description of study area

Guiyang city, capital of Guizhou Province (106.43°E, 26.35°N, 1250 m above MSL), is located on the eastern slope of the Yunnan–Guizhou Plateau, within the highland transition zone in China, surrounded by mountains (Fig. 1). It has a subtropical monsoon climate, with an annual average temperature of 15.3 °C, annual rainfall of 1174 mm, and relative humidity of about 77%. More than a half of the total rainfall occurs in the summer, while less than 10% of the annual rainfall occurs in winter. During the study period, the longest time without rain was 14 days. The dominant wind direction was from the northeast in winter, and from the southeast in summer, with an annual average wind speed of 2.2 m/s from October 2008 to September 2009.

Pollution related to coal combustion has been reduced to some extent in recent years (Xiao et al., 2013). For example, coal-fired household stoves were phased out from 1998, and power plants were moved away from the city (Xiao et al., 2013). These changes led to a 42.1% reduction (from 31×10^7 kg to 17.95×10^7 kg) in total SO₂ emissions (Fig. 2; the data of SO₂ emission from China Environment Statistical Yearbook, 2010), and 59.8% reduction (21×10^7 kg to 8.45×10^7 kg) in industrial SO₂ emissions from 2002 to 2009. This has resulted in a 43.7% decrease in atmospheric SO₂ concentrations (from 0.103 mg/m³ to 0.058 mg/m³) (Fig. 2). Despite this reduction, acid rain still frequently occurs in Guiyang.

2.2. Sampling and chemical analysis

Rainwater samples were collected using two aluminum sheets (7.14 m²) as a collection device, fixed 1.5 m above the roof of a building located at the State Key Laboratory of Environment Geochemistry. The device was cleaned with Milli-Q water and dried before use. The device was kept covered with a large clean polyethylene sheet until it started to rain. Rainwater was collected directly from the device into 1.5 L acid-cleaned plastic bottles. As each bottle was filled, it was replaced manually with a new bottle until the conclusion of the rain. All rainfall events were sampled from the beginning to end over the study period. Thus, a total of 1235 samples were collected between October 2008 and September 2009.

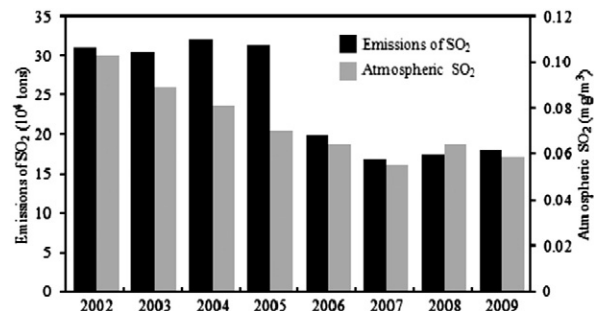


Fig. 2. Anthropogenic SO₂ emission and atmospheric SO₂ concentration from 2002 to 2009 at Guiyang (the data from Guiyang Environment Bulletin, 2003–2010).

After collection, the pH, electrical conductivity (EC), and temperature (T) were immediately measured in a 20 mL subsample from each bottle. The remainder of the sample was passed through a 0.45 μm acetate membrane filter, and refrigerated at 4 °C. A 10 mL subsample was used for SO₄²⁻ concentration analysis and another 1.2 L was used for isotopic analysis (after being treated with HgCl₂). SO₄²⁻ concentrations were measured by ion chromatography (DIONEX ICS-90, Thermo Fisher Scientific Inc., USA), with a 0.1 mg/L detection limit for various ions.

2.3. Isotopic analysis

Sulfur isotopic composition was determined after SO₄²⁻ was separated from the rainwater by anion exchange using anion resin (Dowex® 1-X8, 200-mesh OH⁻ form) at the laboratory. The procedure is described in detail by Xiao and Liu (2002). SO₄²⁻ was eluted with 40 mL of 2 mol/L KCl solution. The sorption efficiency of sulfate was greater than 99.9% (Xiao and Liu, 2002). About 10 mL of this eluent was transferred to a 15 mL centrifuge tube for sulfur isotope analysis. After acidifying with pure HCl solution, the SO₄²⁻ was precipitated as BaSO₄ with 2 mol/L BaCl₂ solution. This mixture was filtered through 0.22 μm acetate membrane filters after 24 h. The precipitate was cleaned with sufficient Milli-Q water to remove Cl⁻ on the filter. The precipitate (BaSO₄) was quickly transferred into crucibles, with the filter, and combusted at 800 °C for 40 min in air.

Sulfur isotopes were determined at the State Key Laboratory of Environment Geochemistry, Institute of Geochemistry. Samples (~500 μg BaSO₄) were accurately weighed into small tin cups (φ3.5 × 5) for analysis. A Eurovector elemental analyzer (EA3000, Eurovector, Italy) was used for on-line combustion of BaSO₄ at 1030 °C and on-line separation of SO₂ to an IsoPrime isotope ratio mass spectrometer for ³⁴S/³²S analyses (IsoPrime Continuous Flow Isotope Ratio Mass Spectrometer, GV Instruments Ltd, UK). This method is described in Grassineau et al. (2001). Each sample was analyzed at least twice. The standard deviation for the δ³⁴S analysis of reference standard NBS127 (BaSO₄) was ±0.2‰ (n = 5). Sulfate concentrations of some samples were lower than 2 mg/L, and thus too low for δ³⁴S analysis. Thus, only about 64% of samples were measured for sulfur isotopes. In summer, fewer samples were analyzed than for other seasons due to greater precipitation amounts, and consequently lower SO₄²⁻ concentrations in rainwater.

2.4. Back-trajectory and concentration weighted trajectory analysis

To identify the influence of long-distance transport of atmospheric SO₂ on the concentration of SO₄²⁻ in rainwater in Guiyang, air mass back trajectories were estimated using TrajStat software (<http://www.arl.noaa.gov/HYSPLIT.php>), with Global Data Assimilation System (GDAS) data provided by the National Oceanic and Atmospheric Administration (NOAA). For each day, a 3-day (72 h) back-trajectory of the air mass arriving at Guiyang, 500 m above ground level, was investigated with time ending at 0 a.m. A cluster analysis was carried out on these back-trajectories (Cape et al., 2000).

To identify impacts of regional source areas on atmospheric SO_4^{2-} concentrations in Guiyang, the concentration weighted trajectory (CWT) or Concentration Field model was used (Stohl, 1996). This model is frequently applied in pollution studies to detect polluted regions that affect the composition at a specified site (Salamalikis et al., 2014). Our CWT model was a function of the SO_4^{2-} concentrations for each rainy day, and one air mass back-trajectory generated for the same day, yielding 144 back-trajectories between October 2008 and September 2009 (Fig. 1). Based on the longest distance traveled by the air mass back-trajectories over the study period, a geographic region from 90 to 130°E and from 15 to 45°N was defined as the source domain. This domain was divided into 2400 grid cells, each covering an area of 0.5° by 0.5°. The CWT for SO_4^{2-} for the grid cells (i, j) in this domain is a measure of the source strength of a grid cell with respect to Guiyang and is defined by (Eq. (1); Cheng et al., 2013):

$$C_{ij} = \frac{1}{\sum_{l=1}^M \tau_{ijl}} \sum_{l=1}^M C_l \tau_{ijl} \quad (1)$$

where C_{ij} is the average weighted concentration of SO_4^{2-} in the ij th cell; l is the index of the trajectory; C_l is the volume-weighted mean SO_4^{2-} concentration from rainwater samples, corresponding to the arrival of back-trajectory l at the sampling site; τ_{ijl} is the time spent in the ij th cell by trajectory l ; and M is the total number of back trajectories.

Although CWT is a powerful tool for atmospheric source identification and has been widely used in many previous studies (e.g. Cheng et al., 2013), there are no studies for sulfur isotopes. Hence, we also tried to use CWT for $\delta^{34}\text{S}$ values in this study. This calculation is analogous to the weighting method used for daily $\delta^{34}\text{S}$, where the weighting factors are the precipitation amount, and SO_4^{2-} concentration. In this calculation, C_l becomes the volume-weighted mean $\delta^{34}\text{S}$ from rainwater samples in Eq. (1) (instead of SO_4^{2-} concentration), and C_{ij} is the average weighted $\delta^{34}\text{S}$ in the ij th cell. CWT plots for SO_4^{2-} and $\delta^{34}\text{S}$ were determined for each season in the 2008 and 2009. The CWT method provided a spatial pattern of the potential sources that contributed to the observed

SO_4^{2-} and $\delta^{34}\text{S}$ at the sampling site. The weighted values at each grid cell obtained from Eq. (1) represent SO_4^{2-} and $\delta^{34}\text{S}$ values that can be expected at the receptor site, if an air parcel would have traveled through the spatial grid. The CWT model was intended to identify regional source areas, but not global or local ones. One of the major sources of uncertainty in the CWT model is the back-trajectory modeling. Wind field errors, modeling of vertical motion, turbulence, and starting position all contribute to trajectory uncertainties (Cheng et al., 2013). Furthermore, the CWT model cannot differentiate between source areas associated with surface emissions and those associated with point sources (Cheng et al., 2013).

2.5. Meteorological parameters

Meteorological data, including air temperature, relative humidity, wind direction and wind speed were measured per minute at the sampling site over the study period.

3. Results and discussion

3.1. General characteristics of rainwater sulfate

The SO_4^{2-} concentrations in rainwater ranged from 0.7 mg/L to 414.6 mg/L (Supplementary material), with a volume-weighted mean of 12.8 mg/L over the study period (Table 1). The SO_4^{2-} concentrations showed obvious seasonal variation (Fig. 3a); they were about 8.2 times higher in winter than in summer. This seasonal variation may be linked to rainfall volume (Xiao et al., 2013), since a negative natural logarithmic relationship was found between SO_4^{2-} concentrations and precipitation ($y = -(13.1 \pm 2.7)\ln x + (71.9 \pm 10.8)$; $R = 0.85$, $P < 0.01$). However, the amount of wet-deposited sulfate was anti-correlated with sulfate concentration, with high values in summer and low values in winter (Fig. 3a).

The SO_4^{2-} concentrations in rainwater decreased from 19.7 mg/L to 12.8 mg/L over the time period from 1982 to 2009 (Zhao et al., 1988; Xiao et al., 2013), mainly due to phasing out of traditional and industrial coal-combustion pollution in the city in recent years (Xiao et al., 2013). The average SO_4^{2-} concentration was still much higher in

Table 1
Temporal variations of weather conditions at Guiyang.

Month	Sampling number	SO_4^{2-} ($\text{mg}\cdot\text{L}^{-1}$)	$\delta^{34}\text{S}$ (‰)	$\delta^{34}\text{S}$ (AF) (‰)	Temperature (°C)	Humidity (%)	Precipitation (mm)	Sunshine ($\text{hr}\cdot\text{day}^{-1}$)
2008.10	159	17.4	-4.1 ± 1.7	-4.2	16.6	82	57.1	2.1
2008.11	63	8.1	-3.7 ± 2.3	-3.9	10.5	72	61.6	2.3
2008.12	24	50.2	-0.9 ± 1.8	-1.0	6.4	76	14.0	1.9
2009.1	25	45.2	-0.8 ± 1.3	-0.9	3.8	73	11.2	1.5
2009.2	49	28.8	-2.4 ± 1.6	-2.4	7.7	77	24.2	2.3
2009.3	43	23.5	-1.7 ± 1.4	-1.7	11.4	71	31.5	2.6
2009.4	156	6.1	-2.6 ± 2.4	-2.7	14.6	77	225.0	1.4
2009.5	112	14.4	-5.3 ± 3.7	-5.4	18.6	76	81.8	2.3
2009.6	139	19.8	-2.6 ± 1.9	-2.6	21.6	73	116.2	2.1
2009.7	238	7.8	-4.1 ± 2.2	-4.2	22.8	76	158.5	3.1
2009.8	140	10.6	-2.7 ± 3.5	-2.9	23.7	69	80.7	4.9
2009.9	87	12.4	N.D.	N.D.	21.7	67	31.7	5.3
Average		12.8	-2.8 ± 9.8	-2.9	15.0	74	74.5	2.6

The data of temperature, humidity, and sunshine is from Xiao et al., (2012). AF: anthropogenic fraction. N.D. means no data.

Guiyang, than in other southern Chinese cities, as well as other countries, e.g., 3.1 mg/L in Shenzhen and 8.0 mg/L in Guangzhou, both in South China; 2.5 mg/L in Tokyo, Japan; 1.9 mg/L in Swargate, India; 0.05 mg/L in Cuiabá, Brazil; and 1.8 mg/L in Adirondack, USA (Cao et al., 2009; Okuda et al., 2005; Ito et al., 2002; Huang et al., 2010; Budhavant et al., 2011; Dias et al., 2012). However, it was lower than those in northern Chinese cities, such as Xi'an (24.0 mg/L; Lu et al., 2011), and Beijing (15.4 mg/L; Yang et al., 2012).

The $\delta^{34}\text{S}$ values in rainwater samples ranged from -12.0% to $+9.4\%$ (Supplementary material), with a volume-weighted mean of $-2.8 \pm 9.8\%$ (Table 1). The higher $\delta^{34}\text{S}$ values were

associated with higher SO_4^{2-} concentrations in winter, and lower $\delta^{34}\text{S}$ values with lower SO_4^{2-} concentrations in summer (Fig. 3b, Xiao et al., 2013). Seasonal variation had a strong sinusoidal pattern ($y = -2.7 + 1.5 \sin(\frac{2\pi}{8.7}x - 1.6)$; Fig. 3b). The volume-weighted means of samples collected at night (18:00–6:00) and during the day (6:00–18:00) were similar ($-2.9 \pm 2.6\%$ and $-2.8 \pm 2.2\%$, respectively). Although, there was a slight difference between day and night samples for summer rain, with $-3.6 \pm 2.4\%$ (n = 100) for night and $-2.8 \pm 2.1\%$ (n = 159) for day samples. The average $\delta^{34}\text{S}$ value of all 1235 samples in Guiyang was close to that for Guilin and Liuzhou Guangxi Provinces in South China (-3.5%

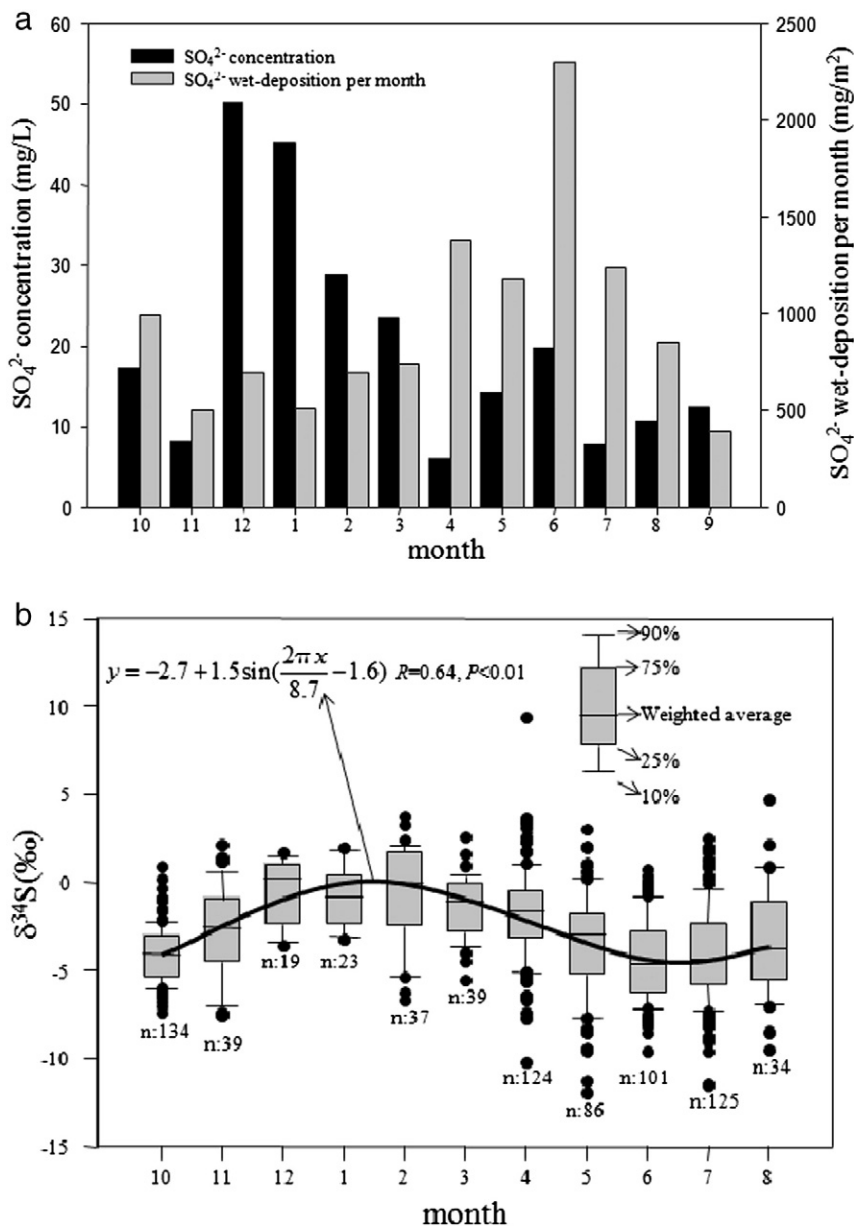


Fig. 3. a: Monthly concentration of sulfate and sulfate wet-deposition per month. b: Monthly variations of $\delta^{34}\text{S}$ in rainwater from Oct. 2008 and Aug. 2009 (n means the number of $\delta^{34}\text{S}$ in rainwater). The lower boundary of the box indicates the 25th percentile, a line within the box marks the average value, and the upper boundary of the box indicates the 75th percentile. Whiskers (error bars) above and below the box indicate the 90th and 10th percentiles.

and -2.8% , respectively; Zhang et al., 2002), suggesting that they may have a similar sulfur source. Previous studies (e.g. Xiao and Liu, 2002; Zhang et al., 2010) reported that the largest contributor to SO_4^{2-} in rainwater was SO_2 emissions from coal combustion in most of Chinese cities. Mukai et al. (2001) also reported that in Guiyang, the $\delta^{34}\text{S}$ values of atmospheric SO_2 and SO_4^{2-} were close to those for coals used in these regions. The same observation was made in Fukuoka, Japan, where the $\delta^{34}\text{S}$ value of atmospheric SO_2 was close to that of local fossil fuel (Kawamura et al., 2001). Compared with southern Chinese cities, the $\delta^{34}\text{S}$ values in northern China cities were more positive, e.g., Xi'an ($+13.4\%$, Bai and Wang, 2014) and Beijing ($+6.8\%$, Hong et al., 1994). These differences in $\delta^{34}\text{S}$ values were ascribed to the different $\delta^{34}\text{S}$ values of regional coals, e.g., the mean $\delta^{34}\text{S}$ values of northern regional coals were: $+12.5\%$ in Shaanxi Province, $+10.0\%$ in Shanxi Province, $+12.1\%$ in Hebei Province, and $+10.7\%$ in Gansu Province (Xiao et al., 2011); while the mean $\delta^{34}\text{S}$ values of southern regional coals were -7.5% in Guizhou Province, -5.7% in Jiangxi Province, and $+1.8\%$ in Hunan Province (Hong et al., 1992; Xiao et al., 2011). In this study, the $\delta^{34}\text{S}$ values of SO_4^{2-} in rainwater were slightly higher than those for local coals (-7.5% ; Hong et al., 1992), suggesting that in addition to sulfur derived from the local combustion of coal, there are other sources, such as biological sources, sea spray or regionally-transported sources from North China that affect the $\delta^{34}\text{S}$ values of SO_4^{2-} in rainwater in Guiyang.

Fig. 4 shows an increase in $\delta^{34}\text{S}$ values of rainwater SO_4^{2-} of about $+0.16\%$ per year in Guiyang from 1987 to 2009, whereas the local anthropogenic SO_2 emissions from ^{34}S -depleted coal combustion have gradually decreased by about 10,000 tons per year since 1987 (Figs. 2 and 4). Interestingly, the same trend was observed in the north-western region of the Czech Republic (Novák et al., 2001), where local SO_2 emissions were reduced, and other unknown sources had higher $\delta^{34}\text{S}$ values than those of local coals.

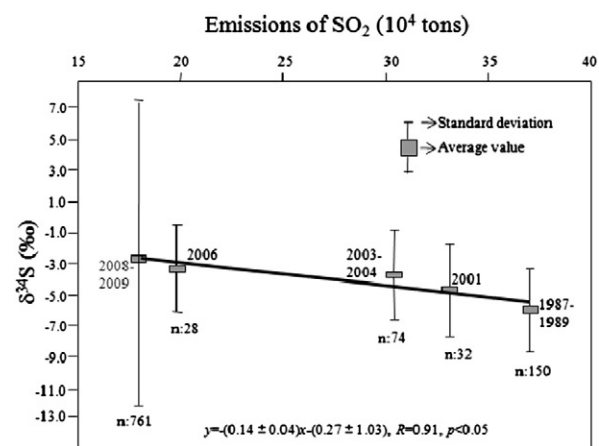


Fig. 4. Relationship between $\delta^{34}\text{S}$ in rainwater and emission of SO_2 from 1987 to 2009 at Guiyang (n means the number of $\delta^{34}\text{S}$ in rainwater; emission of SO_2 from Guiyang Environment Bulletin, 2001, 2003, 2004, 2006, 2008, and 2009; $\delta^{34}\text{S}$ in 1987–1989, in 2001, in 2003–2004 and in 2006 from Hong et al., 1994; Xiao and Liu, 2002; Liu, 2007 and Xiao et al., 2009, respectively).

3.2. Seasonal variation of sources

Winter months were associated with isotopically heavier sulfur than summer months (Fig. 3b). Similar results were reported in Jiangxi, China (Pan et al., 2008), USA (Zhang et al., 1998), Japan (Ohizumi et al., 1997), and Canada (Nriagu and Coker, 1978). The difference in $\delta^{34}\text{S}$ values for winter and summer months was about 3.3% in Guiyang. Nriagu and Coker (1978) also found that the $\delta^{34}\text{S}$ values during cold months were higher by about 4% in the Great Lakes Basin (USA and Canada). In Central Europe, however, lower $\delta^{34}\text{S}$ values were found in winter months, because there was a higher demand for electricity for heating during the cold season, leading to higher anthropogenic SO_2 (isotopically lighter sulfur) emission rates (Novák et al., 2001). Seasonal variation of $\delta^{34}\text{S}$ values in rainwater reflected seasonal changes in sulfur sources, oxidation pathways, scavenging ratio and/or sulfur isotope fractionation taking place in the atmosphere (Harris et al., 2013a; Nriagu and Coker, 1978). It cannot be caused by the seasonal variations in coal combustion in Guiyang (Hong et al., 1994), since there were no differences in the isotopic composition of SO_2 during summer ($-4.5 \pm 4.0\%$) and winter ($-4.1 \pm 2.0\%$) (Mukai et al., 2001).

3.2.1. Sea salt and crust fractions

Since contributions of sulfur from volcanic sources were negligible (there are no volcanoes near Guiyang), the sulfur sources in rainwater must be derived from anthropogenic sources, sea spray, and terrestrial dust (Zhang et al., 2007; Cao et al., 2009). To derive these fractions, Na^+ and Ca^{2+} were taken as reference elements, assuming that all Na^+ originates from marine sources and all Ca^{2+} from terrestrial dust (Zhang et al., 2007; Cao et al., 2009). The sea salt fraction (SSF), crust fraction (CF), and anthropogenic fraction (AF) were calculated using Eqs. (2), (3) and (4), respectively:

$$\text{SSF}(\%) = 100 \left(\frac{X/\text{Na}^+}{(X/\text{Na}^+)_{\text{rainwater}}} \right)_{\text{sea}} \quad (2)$$

$$\text{CF}(\%) = 100 \left(\frac{X/\text{Ca}^{2+}}{(X/\text{Ca}^{2+})_{\text{rainwater}}} \right)_{\text{soil}} \quad (3)$$

$$\text{AF}(\%) = 100 - \text{SSF} - \text{CF} \quad (4)$$

where X represents the SO_4^{2-} concentration.

The approximate contributions of sea salt and crust sources to rainwater SO_4^{2-} are shown in Fig. 5. The SSF for Guiyang samples was $0.60 \pm 0.22\%$, with no obvious seasonal variation, indicating that the contributions of sea salt were consistently very low. This was comparable to other local cities, such as Chengdu, which had a SSF of 0.8% (Wang and Han, 2011). In contrast, total SO_4^{2-} in Erzgebirge and Freiberg regions of Germany comprised $95\text{--}99\%$ non-marine SO_4^{2-} (Zimmermann et al., 2006). These inland cities showed very different SSF to cities close to the coast with a large maritime contribution (Xiao et al., 2014). The CF for Guiyang samples was $1.87 \pm 0.52\%$; it was slightly higher in winter and spring than in summer and autumn, suggesting that there was a small contribution to the seasonal variation from crustal sources. The low CF was consistent with the low sulfur content of local soils (Guan et al., 2013). Contributions of SO_2 from biomass burning in Guizhou and biogenic sulfur were

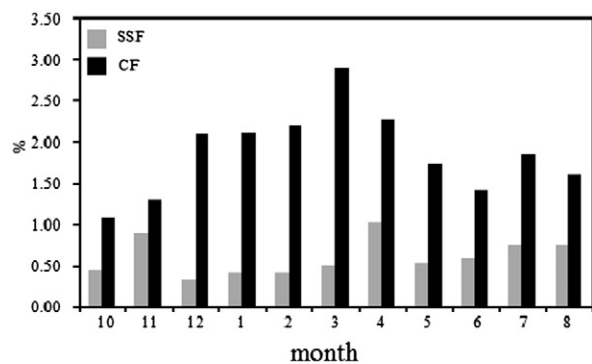


Fig. 5. Monthly percentage of SSF (sea salt fraction) and CF (crust fraction) sources of SO_4^{2-} in rainwater.

neglected (Streets et al., 2003; Yang et al., 1996). Biomass burning in Guizhou accounted for only about 250 tons (Streets et al., 2003) and biogenic sulfur for about 322 tons (Yang et al., 1996), compared with 19.5×10^4 tons for anthropogenic sulfur per year. Thus, anthropogenic sources accounted for about 97.53% of the total SO_4^{2-} . Since $\delta^{34}\text{S}$ of seawater was +21.0‰ (Rees et al., 1978) and the $\delta^{34}\text{S}$ of crust in Guiyang was -2.2‰ (Liu et al., 1996a, 1996b), the $\delta^{34}\text{S}$ of the anthropogenic fraction (AF) was calculated by subtracting from these components.

3.2.2. Trajectory clusters and CWT results

The daily sulfate concentrations (volume-weighted mean concentrations of every day) ranged from 2.9 mg/L to 316.3 mg/L, with an arithmetic average of 41.0 mg/L. Fig. 1 shows the results of the cluster analysis of anthropogenic SO_2 emissions in 2009. Cluster 1 from northwest Hunan Province accounted for 38.8% of trajectories; cluster 2 from the junction of Guangxi Province and Guizhou Province accounted for 12.5% of trajectories; cluster 3 from west Guangxi Province accounted for 28.5% of trajectories; while clusters 4, 5, and 6 accounted for less than 10% of all trajectories. These clusters suggest that the external source of sulfur in Guiyang was from the region covered by Guizhou–Guangxi–Hunan Provinces. These three provinces had similar SO_2 emission intensities, with 6.7×10^3 kg/km² in Guizhou, and 3.8×10^3 kg/km² in Guangxi and Hunan Provinces (data from China Environment Statistical Yearbook, 2010, Fig. 1). Among these three provinces, the SO_2 emission intensity in Guizhou was highest, about 1.76 times greater than that in Guangxi and Hunan Provinces. The SO_2 concentrations in the capital cities of these provinces were 0.058 mg/m³ in Guiyang (Guizhou), 0.032 mg/m³ in Nanning (Guangxi), and 0.039 mg/m³ in Changsha (Hunan) (data from China Environment Statistical Yearbook, 2010). Again, values in Guiyang were 1.81 and 1.49 times higher than that in the other two cities, respectively.

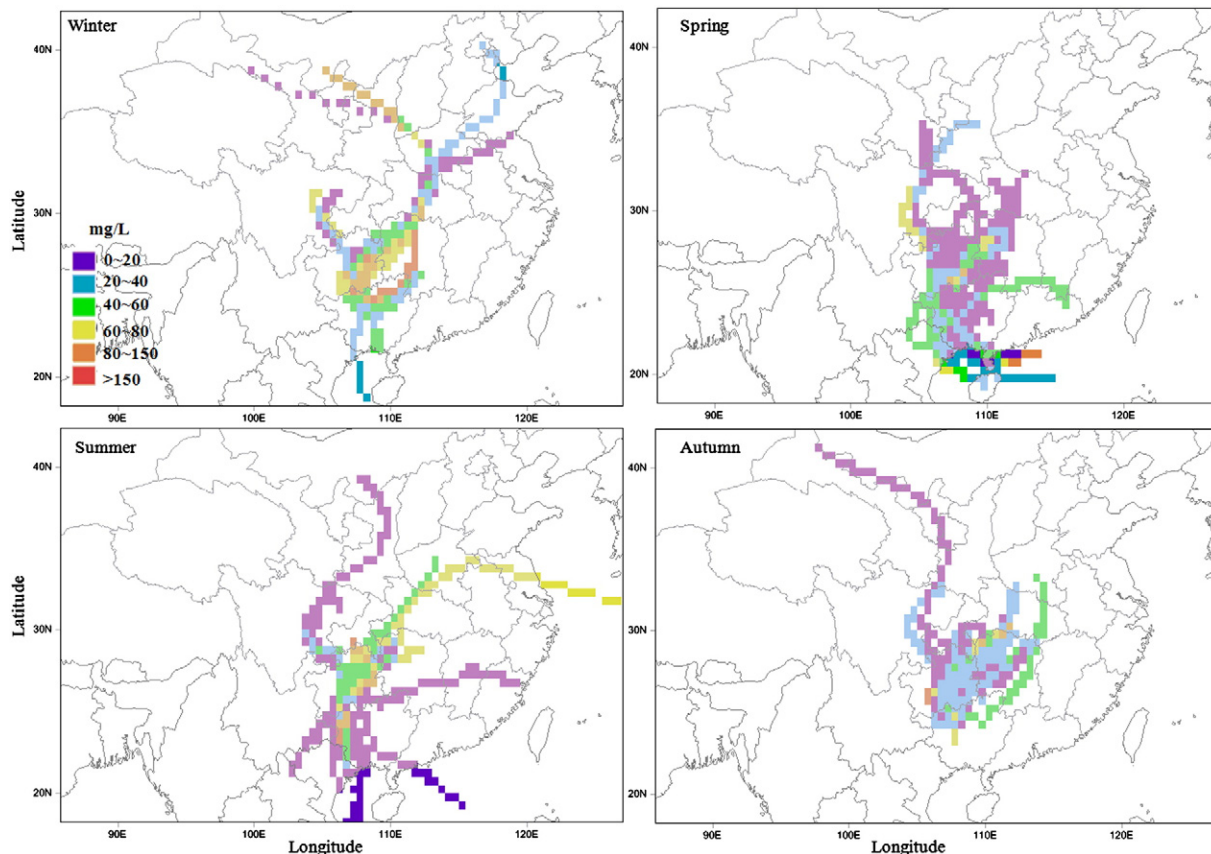


Fig. 6. Different seasonal CWT (concentration weighted trajectory) plots for daily weighted average concentrations of daily weighted average values of SO_4^{2-} .

The CWT plotted for SO_4^{2-} is shown in Fig. 6. The winter CWT plots for SO_4^{2-} indicate that east Guizhou, north Guangxi, and northwest Hunan are likely source regions of rainwater SO_4^{2-} in Guiyang. In addition, there is a component of long-distance transported SO_4^{2-} from north and northwest regions of China with high SO_4^{2-} (Bai and Wang, 2014). In winter, the daily SO_4^{2-} concentrations in Guiyang varied greatly, reaching concentrations higher than 60 mg/L on some days. The spring CWT plots show that the source regions were likely a large area formed by central and eastern Guizhou, west Guangxi, and west Hunan Provinces. The summer CWT plots indicate that central and eastern Guizhou, northwest Hunan and north Guangxi Provinces, as well as the northern region of the South China Sea were likely source regions in this season. The autumn CWT plots show that the source regions were likely a region formed by central and eastern Guizhou and Hunan Provinces.

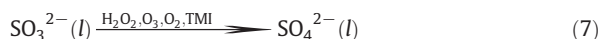
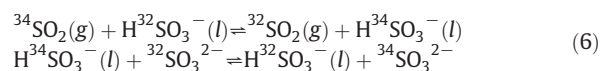
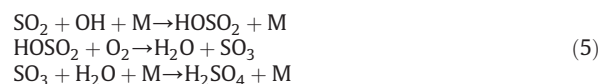
To identify sulfur sources, seasonal CWT plots for $\delta^{34}\text{S}$ were also calculated (Fig. 7). They show that that high $\delta^{34}\text{S}$ values were generally from the north in winter, and low $\delta^{34}\text{S}$ values from the south in summer. Hong et al. (1994) reported that the rainwater SO_4^{2-} was ^{34}S -enriched north of the Yangtze River, while ^{34}S -depleted south of the Yangtze River; they attributed these isotopic differences to the differences in $\delta^{34}\text{S}$ of local coals. In Guiyang, we found a relationship between $\delta^{34}\text{S}$ and $1/\text{SO}_4^{2-}$ in winter ($R = 0.5$, $P = 0.01$), but no correlation was found in other seasons ($R = 0.3$, $P \gg 0.05$ for spring; $R = 0.1$, $P \gg 0.05$ for summer; $R = 0.1$, $P \gg 0.05$ for autumn, respectively), suggesting that the $\delta^{34}\text{S}$ and SO_4^{2-} concentrations were significantly affected by the sources in North China during winter.

3.3. Seasonal variation in isotopic composition

Both isotopic fractionation and seasonal variation in sulfate source were important factors affecting the seasonal variation in sulfur isotopic composition in the atmosphere. The isotopic composition of secondary sulfates depended largely on the isotopic composition of the precursor SO_2 , as well as oxidation processes in the atmosphere. Thus, oxidation of SO_2 to SO_4^{2-} had a significant effect on isotopic composition (Novák et al., 2000, 2001; Harris et al., 2012a, 2013a).

Oxidation of SO_2 has two pathways, involving homogeneous or heterogeneous oxidation (Novák et al., 2001). Homogeneous oxidation only involves kinetic fractionation, whereas the heterogeneous pathway involves both equilibrium and kinetic fractionation (Harris et al., 2012a, 2013a). The product, H_2SO_4 , formed from homogeneous oxidation can stick to the surfaces of existing particles or nucleates to form new particles in the atmosphere, which grow to act as cloud condensation nuclei (Eq. (5); Benson et al., 2008; Harris et al., 2012a; Kulmala et al., 2004). Heterogeneous oxidation occurs under aqueous or dry conditions; dry heterogeneous oxidation is rare under most atmospheric conditions (Usher et al., 2002; Ullerstam et al., 2002; Al-Hosney and Grassian, 2005; Harris et al., 2012b). Aqueous oxidation takes place within solutions or fluid films on wetted surfaces of particles; it involves dissolution of SO_2 by acid-base dissociation of $\text{SO}_2 \cdot \text{H}_2\text{O}(l)$ to $\text{HSO}_3^-(l)$ and $\text{SO}_3^{2-}(l)$, followed by oxidation of SO_3^{2-} and/or HSO_3^- to SO_4^{2-} by

major oxidants, such as H_2O_2 , O_3 , O_2 or transition metal ions (Eqs. (6) and (7); Eriksen, 1972a, 1972b; Herrmann et al., 2000; Harris et al., 2012c; Harris et al., 2013a; Savarino et al., 2000).



In Guiyang, the pH value of cloud water was low (about 4.6; Huang et al., 1995); hence, oxidation was likely dominated by H_2O_2 (Harris et al., 2013a, 2013b). Oxidation by transition metal ions (TMI) results in products depleted in ^{34}S relative to their SO_2 source (Harris et al., 2013a). The catalysis of SO_2 to SO_4^{2-} by TMI is probably underestimated in many cities (Alexander et al., 2009; Harris et al., 2013a). Aqueous oxidation produces SO_4^{2-} on the surface of particles or in droplets, changing their cloud condensation nuclei activity, lifetime, and growth due to their increased hygroscopicity (Mertes et al., 2005). We surmise that aqueous oxidation will be more important in winter than in summer for two reasons: (1) photochemical production of gaseous oxidants is greatest during summer, and (2) SO_2 solubility decreases with increasing temperature (Eriksen, 1972a, 1972b; Saltzman et al., 1983). Therefore, aqueous oxidation likely played a dominant role during winter (Saltzman et al., 1983).

Fractionation with respect to the source SO_2 was given by $8.9 \pm 0.7 - (4 \pm 5) \times 10^{-2} T$ ($^\circ\text{C}$) for homogeneous oxidation (involving OH), and $(16.7 \pm 1.9) - (8.7 \pm 3.5) \times 10^{-2} T$ ($^\circ\text{C}$) for aqueous oxidation (involving H_2O_2 or O_3) (Harris et al., 2012a); hence, both oxidations by OH and H_2O_2 were temperature-dependent. Furthermore, temperature-dependent isotopic fractionation was also found for oxidation via the catalysis pathway (with a fractionation factor: $(-5.039 \pm 0.044) - (0.237 \pm 0.004) \times T$ ($^\circ\text{C}$; Harris et al., 2013a).

3.3.1. Temperature effects on oxidation pathways

Saltzman et al. (1983) compared $\delta^{34}\text{S}$ values of atmospheric SO_2 and particulate SO_4^{2-} , deducing that mainly homogeneous oxidation of SO_2 occurred in Hubbard Brook Environmental Forest, USA. In South China, aqueous oxidation of SO_2 was believed to occur in the atmosphere (e.g. Zhang et al., 2010) because of its high relative humidity (Xiao et al., 2012). Aqueous-phase reactions in cloud and fog droplets, or in films on wetted particle surfaces, were also described using the aqueous oxidation pathway (Tichomirowa and Heidelberg, 2012). However, seasonal temperatures have a strong sinusoidal pattern in Guiyang ($y = -2.7 + 1.5 \sin(\frac{2\pi}{87}x - 1.6)$; $R = 0.99$, $P < 0.0001$; Xiao et al., 2012), opposite to the $\delta^{34}\text{S}$ seasonal variation ($y = -2.7 + 1.5 \sin(\frac{2\pi}{87}x - 1.6)$; Fig. 3b). Thus, a negative linear relationship was found between temperature and $\delta^{34}\text{S}$ (Fig. 8), not only in Guiyang (data from Hong et al., 1994, and 2008–2009), but also in Guangzhou (data from Zhang et al., 2002), indicating that enrichment was low under high summer temperatures in South China. Some scientists

suggest that temperature could affect sulfur isotopic fractionation, and oxidation pathways (Eriksen, 1972a, 1972b; Saltzman et al., 1983; Harris et al., 2013b). Under low temperatures, dissolution of SO_2 is the rate-limiting step between gaseous and aqueous phases (Eq. (6)), and results in isotopic fractionation with a fractionation factor >1 (Harris et al., 2013b). This sulfur equilibrium fractionation leads to a heavier product with decreasing temperature, with enrichment of 0.08–0.145‰ per 1°C (Saltzman et al., 1983; Caron et al., 1986; Harris et al., 2012a). Thus, $^{34}\text{SO}_2$ would preferentially join the aqueous-phase, resulting in depletion of ^{34}S in the remaining atmospheric SO_2 and enrichment of ^{34}S in SO_4^{2-} (Eq. (6)). Under higher temperatures, the catalytic chain reaction is the rate-limiting step with strong kinetic fractionation favoring the lighter isotope (Harris et al., 2013b).

3.3.2. Oxidation in summer

In summer, homogeneous oxidation by OH involves preferential oxidation of the heavy isotope, causing atmospheric SO_2 to be ^{34}S -depleted by nearly 3‰ (Harris et al., 2013b). In summer, the $\delta^{34}\text{S}$ values of atmospheric SO_2 in Guiyang were $-4.5 \pm 4.0\text{‰}$, which is lower than those of SO_4^{2-} in particulate aerosols by about 3.2‰ (Mukai et al., 2001). In our study, summer $\delta^{34}\text{S}$ was higher during the day ($-2.8 \pm 2.1\text{‰}$) than at night ($-3.6 \pm 2.4\text{‰}$), suggesting

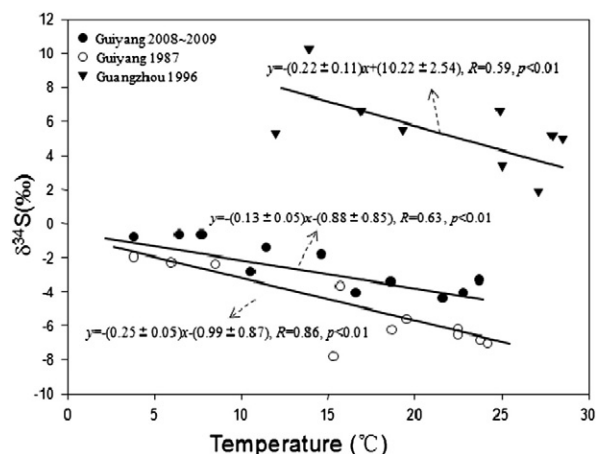


Fig. 8. Relationship between monthly $\delta^{34}\text{S}$ values and monthly temperature in 1987 (data from Hong et al., 1994) and 2008–2009 at Guiyang (Oct. 2008 to Aug. 2009), and in 1996 at Guangzhou (monthly $\delta^{34}\text{S}$ values of Guangzhou from Zhang et al., 2002; temperature of Guangzhou from Guangzhou Bureau of Statistics, <http://www.gzstats.gov.cn/>).

that oxidation by OH mainly took place in daylight hours (at higher temperatures); oxidation by TMI played a more important role at night (at lower temperatures), resulting in a higher proportion of oxidized SO_2 (Harris et al., 2013b).

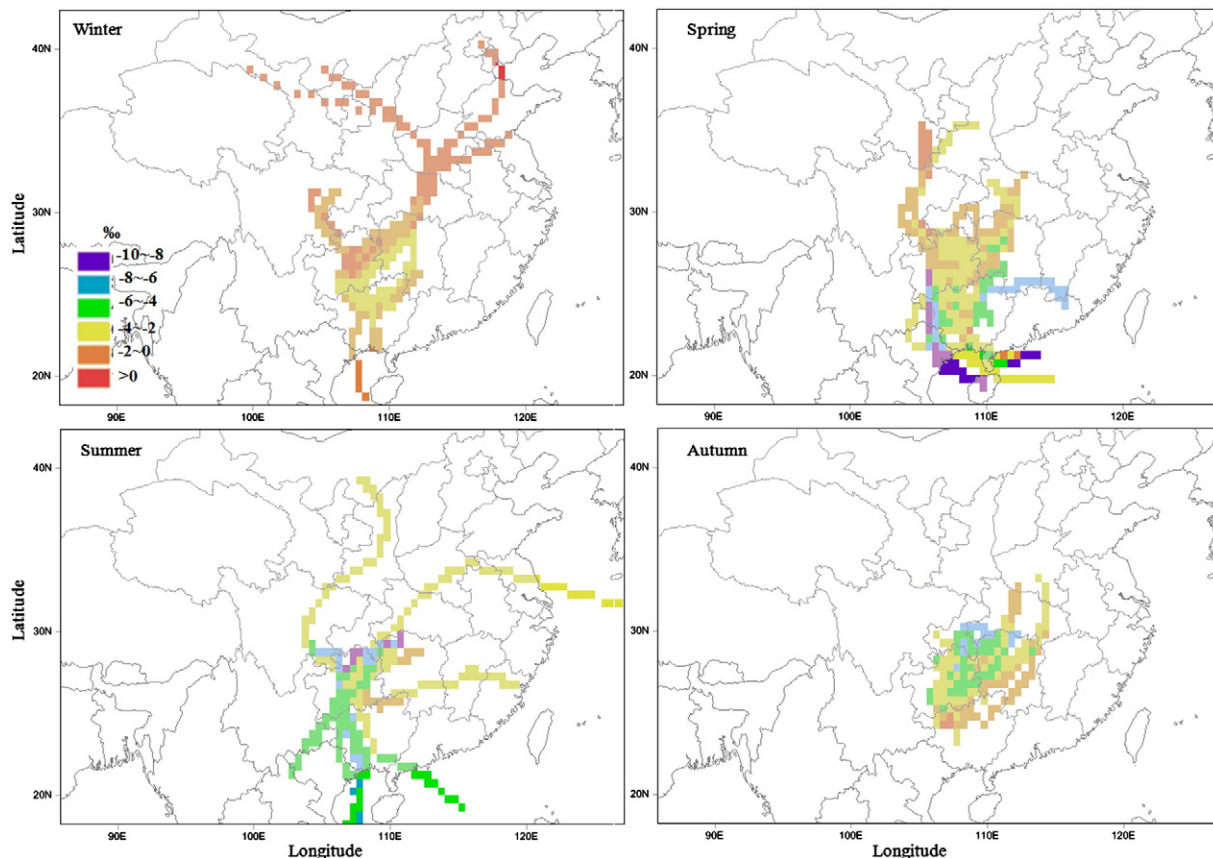


Fig. 7. Different seasonal CWT (concentration weighted trajectory) plots for daily weighted average concentrations of daily weighted average values of $\delta^{34}\text{S}$.

Both processes and sources caused the $\delta^{34}\text{S}$ of atmospheric sulfate in summer to be lighter than that in winter. This pattern also has been reported from sites in the USA (Zhang et al., 1998), Japan (Ohizumi et al., 1997), and Canada (Nriagu and Coker, 1978).

3.3.3. Isotopic fractionation during washout processes

Few studies have been carried out on sulfur isotopic fractionation during washout processes, involving the removal of aerosol particles and soluble gases by raindrops below cloud. Xiao et al. (2010) reported that coarse mode particles were first removed by rain droplets, followed by fine mode particles, and SO_2 in Guiyang. Sulfur in these coarse particles was mainly primary SO_4^{2-} , formed before being released into the atmosphere, e.g., from weathered soils or combustion processes (Liu et al., 1996a, 1996b; Tichomirowa and Heidel, 2012). Fig. 9 shows that during a 13.4 mm rain event on 31 October 2008, SO_4^{2-} concentrations were much higher in the initial 4.5 mm of precipitation than in those that followed, suggesting that the removal of coarse aerosol particles was immediate and effective. Generally, sulfur in the coarse particles, fine particles, and SO_2 had different $\delta^{34}\text{S}$ values (Liu et al., 1996a, 1996b). Since coarse aerosol particles in Guiyang were derived from soils and coal combustion, $\delta^{34}\text{S}$ values of sulfur in these particles were -2.2% and -2.3% , respectively, (Liu et al., 1996a, 1996b; Zhang et al., 2010). In our study, an average $\delta^{34}\text{S}$ value of -3.6% was found for rainwater SO_4^{2-} (Fig. 9), which was lower than that for coarse particles, possibly because it also captured fine particles and SO_2 at the same time. In the later stage of this rain event, we surmise that more fine particles and SO_2 were captured by rain droplets, since they had a lower removal efficiency than coarse particles (Xiao et al., 2010). The sulfur isotope equilibrium fractionation factor was 1.0165 in the aqueous phase at 25°C (Winterholler et al., 2008), so ^{34}S was preferentially incorporated into raindrops by exchange reactions, leaving the lighter isotope in the atmosphere (Fig. 9). Compared with other rain events recorded in

this study, relatively more stable meteorological conditions for temperature ($13.1 \pm 0.4^\circ\text{C}$), intensity ($2.4 \pm 1.6\text{ mm/h}$), wind direction (44.2 ± 14.0) and speed ($2.8 \pm 0.7\text{ m/s}$) occurred for the 31 Oct. 2008 rain event, suggesting that the washout effect was more pronounced under stable meteorological conditions.

4. Conclusions

Volume-weighted mean SO_4^{2-} concentrations and $\delta^{34}\text{S}$ values in rainwater in Guiyang over the year-long study period were 12.8 mg/L and -2.8% , respectively; both variables were higher in winter than in summer. Seasonal variation in $\delta^{34}\text{S}$ values was strongly sinusoidal, suggesting that changes to sources, isotopic fractionation mechanisms, and oxidation pathways took place. In winter, some of the isotopically heavy sulfur in the rainwater was derived from North China, while in summer isotopically light sulfur came from South China. However, the dominant sulfur in rainwater in Guiyang was isotopically light, mainly derived from local coal combustion sources. Isotope signatures suggest that temperature-dependent aqueous oxidation was the major oxidation process of SO_2 in Guiyang, resulting in lower rainwater $\delta^{34}\text{S}$ values under higher temperatures. Furthermore, both washout processes and precipitation volumes were important factors, affecting the seasonal variation of rainwater $\delta^{34}\text{S}$ in Guiyang.

Acknowledgments

This study work was kindly supported by the National Natural Science Foundation of China through Grants 41203015 (H.-W. Xiao), 41273027, 41173027 (H.-Y. Xiao), and 40721002 (C.-Q. Liu), as well as the Strategic Priority Research Program of the Chinese Academy of Sciences through Grants XDA11030103 and XDA11020202.

Appendix A. Supplementary data

Supplementary data to this article can be found online at <http://dx.doi.org/10.1016/j.atmosres.2014.06.003>.

References

- Al-Hosney, H.A., Grassian, V.H., 2005. Water, sulfur dioxide and nitric acid adsorption on calcium carbonate: a transmission and ATR-FTIR study. *Phys. Chem. Chem. Phys.* 7, 1266–1276.
- Alexander, B., Park, R.J., Jacob, D.J., Gong, S., 2009. Transition metal-catalyzed oxidation of atmospheric sulfur: global implications for the sulfur budget. *J. Geophys. Res.-Atmos.* 114. <http://dx.doi.org/10.1029/2008JD010486>.
- Amrani, A., Said-Ahmad, W., Shaked, Y., Kiene, R., 2013. Sulfur isotope homogeneity of oceanic DMSP and DMS. *PNAS*. <http://dx.doi.org/10.1073/pnas.1312956110>.
- Andreae, M.O., 1990. Ocean-atmosphere interactions in the global biogeochemical sulfur cycle. *Mar. Chem.* 30, 1–29.
- Andreae, M.O., Jones, C.D., Cox, P.M., 2005. Strong present-day aerosol cooling implies a hot future. *Nature* 435 (7046), 1187–1190.
- Bai, L., Wang, Z.L., 2014. Anthropogenic influence on rainwater in the Xi'an City, Northwest China: constraints from sulfur isotope and trace elements analyses. *J. Geochem. Explor.* 137, 65–72.
- Berglen, T.F., Berntsen, T.K., Isaksen, I.S.A., Sundet, J.K., 2004. A global model of the coupled sulfur/oxidant chemistry in the troposphere: the sulfur cycle. *J. Geophys. Res.-Atmos.* 109. <http://dx.doi.org/10.1029/2003JD003948>.
- Benson, D.R., Young, L.H., Kameel, F.R., Lee, S.H., 2008. Laboratory-measured nucleation rates of sulfuric acid and water binary homogeneous

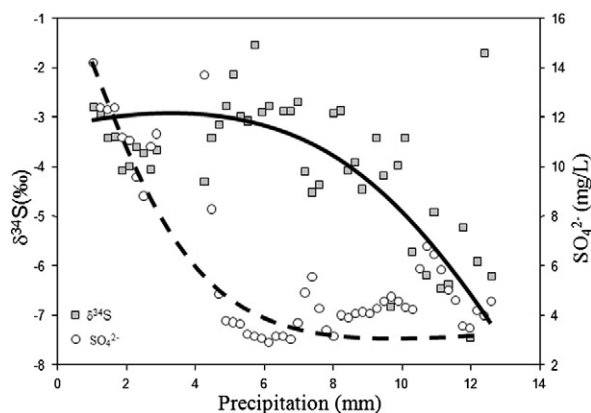


Fig. 9. Variations of $\delta^{34}\text{S}$ and SO_4^{2-} in a 13.4 mm rain event on 2008.10.31 (The solid line and the dashed line mean the trends of $\delta^{34}\text{S}$ and SO_4^{2-} concentrations, respectively.) The average temperature, intensity, wind direction and wind speed were $13.1 \pm 0.4^\circ\text{C}$, $2.4 \pm 1.6\text{ mm/h}$, 44.2 ± 14.0 and $2.8 \pm 0.7\text{ m/s}$, respectively. And every sample was divided by 1.5 L volume.

- nucleation from the $\text{SO}_2^+ \text{OH}$ reaction. *Geophys. Res. Lett.* 35 (11). <http://dx.doi.org/10.1029/2008GL03387>.
- Budhavant, K.B., Rao, P.S.P., Safai, P.D., Ali, K., 2011. Influence of local sources on rainwater chemistry over Pune region, India. *Atmos. Res.* 100, 121–131.
- Calhoun, J.A., Bates, T.S., 1989. Sulfur isotope ratios. Tracers of non-sea salt sulfate in the remote atmosphere. ACS Symposium Series, Biogenic Sulfur in the Environment, 393, pp. 367–379.
- Cao, Y.Z., Wang, S., Zhang, G., Luo, J., Lu, S., 2009. Chemical characteristics of wet precipitation at an urban site of Guangzhou, South China. *Atmos. Res.* 94 (3), 462–469.
- Cape, J.N., Methven, J., Hudson, L.E., 2000. The use of trajectory cluster analysis to interpret trace gas measurements at Mace Head, Ireland. *Atmos. Environ.* 34 (22), 3651–3663.
- Caron, F., Tessier, A., Kramer, J.R., Schwartz, H.P., Rees, C.E., 1986. Sulfur and oxygen isotopes of sulfate in precipitation and lakewater, Quebec, Canada. *Appl. Geochem.* 1, 601–606.
- Cheng, L., Zhang, L., Blanchard, P., Dalziel, J., Tordon, R., 2013. Concentration-weighted trajectory approach to identifying potential sources of speciated atmospheric mercury at an urban coastal site in Nova Scotia, Canada. *Atmos. Chem. Phys.* 13 (12), 6031–6048.
- Dias, V.R.M., Sanches, L., Alves, M.C., Nogueira, J.S., 2012. Spatio-temporal variability of anions in wet precipitation of Cuiabá, Brazil. *Atmos. Res.* 107, 9–19.
- Eriksen, T.E., 1972a. Sulfur isotope effects. I. The isotopic exchange coefficient for the sulfur isotopes ^{34}S – ^{32}S in the system SO_{2g} – $\text{HSO}_3^- \text{aq}$ at 25, 35, and 45 degrees C. *Acta Chem. Scand.* 26, 573–580.
- Eriksen, T.E., 1972b. Sulfur isotope effects. II. The isotopic exchange coefficients for the sulfur isotopes ^{34}S – ^{32}S in the system SO_{2g} –aqueous solutions of SO_2 . *Acta Chem. Scand.* 26, 581–584.
- Galloway, J.N., Zhao, D.W., Xiong, J.L., Likens, G.E., 1987. Acid rain: China, United States, and a remote area. *Science* 236 (4808), 1559–1562.
- Grassineau, N.V., Matthey, D.P., Lowry, D., 2001. Sulfur isotope analysis of sulfide and sulfate minerals by continuous flow-isotope ratio mass spectrometry. *Anal. Chem.* 73, 220–225.
- Guan, H., Xiao, H.Y., Zhu, R.G., Zheng, N.J., Qu, L.L., 2013. Sulfur isotopic signatures in leaves of *Pinus massoniana* Lamb. and source apportionment. *Environ. Sci.* 34 (10), 51–55 (in Chinese with English abstract).
- Harris, E., Sinha, B., Hoppe, P., Crowley, J.N., Ono, S., Foley, S., 2012a. Sulfur isotope fractionation during oxidation of sulfur dioxide: gas-phase oxidation by OH radicals and aqueous oxidation by H_2O_2 , O_3 and iron catalysis. *Atmos. Chem. Phys.* 12 (1), 407–423.
- Harris, E., Sinha, B., Foley, S., Crowley, J.N., Borrmann, S., Hoppe, P., 2012b. Sulfur isotope fractionation during heterogeneous oxidation of SO_2 on mineral dust. *Atmos. Chem. Phys. Discuss.* 12, 2303–2353.
- Harris, E., Sinha, B., Hoppe, P., Foley, S., Borrmann, S., 2012c. Fractionation of sulfur isotopes during heterogeneous oxidation of SO_2 on sea salt aerosol: a new tool to investigate non-sea salt sulfate production in the marine boundary layer. *Atmos. Chem. Phys.* 12, 4619–4631.
- Harris, E., Sinha, B., van Pinxteren, D., Tilgner, A., Fomba, K.W., Schneider, J., Roth, A., Gnauk, T., Fahlbusch, B., Mertes, S., Lee, T., Collett, J., Foley, S., Borrmann, S., Hoppe, P., Herrmann, H., 2013b. Enhanced role of transition metal ion catalysis during in-cloud oxidation of SO_2 . *Science* 340 (6133), 727–730.
- Harris, E., Sinha, B., Hoppe, P., One, S., 2013a. High-precision measurements of ^{33}S and ^{34}S fractionation during SO_2 oxidation reveal causes of seasonality in SO_2 and sulfate isotopic composition. *Environ. Sci. Technol.* 47, 12174–12183.
- Herrmann, H., Ervens, B., Jacobi, H., Wolke, R., Nowacki, P., Zellner, R., 2000. CAPRAM2. 3: a chemical aqueous phase radical mechanism for tropospheric chemistry. *J. Atmos. Chem.* 36 (3), 231–284.
- Herut, B., Spiro, B., Starinsky, A., Katz, A., 1995. Sources of sulfur in rainwater as indicated by isotopic $\delta^{34}\text{S}$ data and chemical composition, Israel. *Atmos. Environ.* 29 (7), 851–857.
- Hong, Y.T., Zhang, H.B., Zhu, Y.X., Piao, H.C., Jiang, H.B., Zeng, Y.Q., Liu, G.S., 1992. Sulfur isotopic characteristics of coal in China and sulfur isotopic fractionation during coal-burning process. *Sci. Sin. Chim.* 22 (8), 868–873 (in Chinese).
- Hong, Y.T., Zhang, H.B., Zhu, Y.X., Piao, H.C., Jiang, H.B., Liu, D.P., 1994. Characteristics of sulfur isotopic composition of meteoric water in China. *Progr. Nat. Sci.* 4, 741–745 (in Chinese with English abstract).
- Huang, M.Y., Shen, Z.L., Liu, S.R., Wu, Y.X., Xiao, H., Lei, H.C., Bai, C.H., 1995. A study on the formation processed of acid rain in some areas of Southwest China. *Sci. Atmos. Sin.* 19 (3), 359–366 (in Chinese with English abstract).
- Huang, X.F., Li, X., He, L.Y., Feng, N., Hu, M., Zeng, L.W., 2010. 5-year study of rainwater chemistry in a coastal mega-city in South China. *Atmos. Res.* 97, 185–193.
- Ito, M., Mitchell, M.J., Driscoll, C.T., 2002. Spatial patterns of precipitation quantity and chemistry and air temperature in the Adirondack region of New York. *Atmos. Environ.* 36 (6), 1051–1062.
- Karnieli, A., Derimian, Y., Indoitu, R., Panov, N., Levy, R.C., Remer, L.A., Maenhaut, W., Holben, B.N., 2009. Temporal trend in anthropogenic sulfur aerosol transport from central and eastern Europe to Israel. *J. Geophys. Res.* 114, D00D19.
- Kawamura, H., Matsuoka, N., Tawaki, S., Momoshima, N., 2001. Sulfur isotope variations in atmospheric sulfur oxides, particulate matter and deposits collected at Kyushu Island, Japan. *Water Air Soil Pollut.* 130 (1–4), 1775–1780.
- Kellogg, W.W., Cadle, R.D., Allen, E.R., Lazrus, A.L., Martell, E.A., 1972. The sulphur cycle: man's contributions are compared to natural sources of sulphur compounds in the atmosphere and oceans. *Science* 175, 587–596.
- Krouse, H.R., Van Everdingen, R.O., 1984. $\delta^{34}\text{S}$ variations in vegetation and soil exposed to intense biogenic sulphide emissions near Paige mountain, N.W.T., Canada. *Water Air Soil Pollut.* 23, 61–67.
- Kulmala, M., Vehkamäki, H., Petäjä, T., Dal Maso, M., Lauri, A., Kerminen, V., Birmili, W., McMurry, P.H., 2004. Formation and growth rates of ultrafine atmospheric particles: a review of observations. *J. Aerosol Sci.* 35 (2), 143–176.
- Li, Y.F., Zhang, Y.J., Cao, G.L., Liu, J.H., Barrie, L.A., 1999. Distribution of seasonal SO_2 emissions from fuel combustion and industrial activities in Shanxi Province, China, with $1/6^\circ \times 1/4^\circ$ longitude/latitude resolution. *Atmos. Environ.* 33, 257–265.
- Liu, C.Q., 2007. Bio-geochemical Processes and Cycling of Nutrients in the Earth's Surface: Erosion of Karstic Catchment and Nutrients Cycling in Southwest China. Science Press, Beijing, pp. 1–608 (in Chinese).
- Liu, G.S., Hong, Y.T., Piao, H.C., Zeng, Y.Q., 1996a. Study on sources of sulfur in atmospheric particulate matter with stable isotope method. *China Environ. Sci.* 16, 426–429 (in Chinese with English abstract).
- Liu, G.S., Hong, Y.T., Piao, H.C., Zeng, Y.Q., 1996b. The sulfur isotopic compositional characteristics of atmospheric particulates from near the ground in the urban and suburban areas of Guiyang city. *Acta Mineral. Sin.* 16, 363–357 (in Chinese with English abstract).
- Liu, Z., Zhang, Q., Streets, D.G., 2011. Sulfur dioxide and primary carbonaceous aerosol emissions in China and India, 1996–2010. *Atmos. Chem. Phys.* 11, 9839–9864.
- Lu, X., Li, L.Y., Li, N., Yang, G., Luo, D., Chen, J., 2011. Chemical characteristics of spring rainwater of Xi'an city, NW China. *Atmos. Environ.* 45, 5058–5063.
- McArdel, N.C., Liss, P.S., 1995. Isotopes and atmospheric sulphur. *Atmos. Environ.* 29, 2553–2556.
- Mertes, S., Lehmann, K., Nowak, A., Massling, A., Wiedensohler, A., 2005. Link between aerosol hygroscopic growth and droplet activation observed for hill-capped clouds at connected flow conditions during FEBUKO. *Atmos. Environ.* 39 (23), 4247–4256.
- Mukai, H., et al., 2001. Regional characteristics of sulfur and lead isotope ratios in the atmosphere at several Chinese urban sites. *Environ. Sci. Technol.* 35, 1064–1071.
- Novák, M., Kirchner, J.W., Groscheová, H., Havel, M., Černý, J., Krejčí, R., Buzek, F., 2000. Sulfur isotope dynamics in two central European watersheds affected by high atmospheric deposition of SO_x. *Geochim. Cosmochim. Acta* 64 (3), 367–383.
- Novák, M., Jac Ková, I., Prechova, E., 2001. Temporal trends in the isotope signature of air-borne sulfur in Central Europe. *Environ. Sci. Technol.* 35 (2), 255–260.
- Nriagu, J.O., Coker, R.D., 1978. Isotopic composition of sulfur in precipitation within the Great Lakes Basin. *Tellus* 30 (4), 365–375.
- Ohizumi, T., Fukuzaki, N., Kusakabe, M., 1997. Sulfur isotopic view on the sources of sulfur in atmospheric fallout along the coast of the Sea of Japan. *Atmos. Environ.* 31, 1339–1348.
- Okuda, T., Iwase, T., Ueda, H., Suda, Y., Tanaka, S., Dokiya, Y., Fushimi, K., Hosoe, M., 2005. Long-term trend of chemical constituents in precipitation in Tokyo metropolitan area, Japan, from 1990 to 2002. *Sci. Total Environ.* 339, 127–141.
- Pan, J., Le, C., Chen, Y., Yan, Z., 2008. Study on sulfur isotopes in rain water in Nanchang, China. *Geochim. Cosmochim. Acta* 72, A721.
- Quinn, P.K., Coffman, D.J., 1998. Local closure during the first Aerosol Characterization Experiment (ACE 1): aerosol mass concentration and scattering and backscattering coefficients. *J. Geophys. Res.* 103, 16575–16596.
- Rotsayn, L.D., Lohmann, U., 2002. Simulation of the tropospheric sulfur cycle in a global model with a physically based cloud scheme. *J. Geophys. Res.* 107. <http://dx.doi.org/10.1029/2002JD002128>.
- Rees, C.E., Jenkins, W.J., Monster, J., 1978. The sulphur isotopic composition of ocean water sulphate. *Geochim. Cosmochim. Acta* 42 (4), 377–381.
- Salamalikis, V., Argiriou, A.A., Dotsika, E., 2014. Stable isotopic composition of atmospheric water vapor in Patras, Greece: a concentration weighted trajectory approach. *Atmos. Res.* <http://dx.doi.org/10.1016/j.atmosres.2014.02.021>.

- Saltzman, E.S., Brass, G.W., Price, D.A., 1983. The mechanism of sulfur aerosol formation: chemical and sulfur isotopic evidence. *Geophys. Res. Lett.* 10, 513–516.
- Savarino, J., Lee, C.C.W., Thiemens, M.H., 2000. Laboratory oxygen isotopic study of sulfur (IV) oxidation: origin of the mass-independent oxygen isotopic anomaly in atmospheric sulfates and sulfate mineral deposits on Earth. *J. Geophys. Res.* 105, 29079–29088.
- Scott, B.C., 1978. Parameterization of sulphate removal by precipitation. *J. Appl. Meteorol.* 17 (9), 1375–1389.
- Scott, B.C., Hobbs, P.V., 1967. The formation of sulphate in water droplets. *J. Atmos. Sci.* 24, 54–57.
- Stohl, A., 1996. Trajectory statistics—a new method to establish source–receptor relationships of air pollutants and its application to the transport of particulate sulfate in Europe. *Atmos. Environ.* 30, 579–587.
- Streets, D.G., Yarber, K.F., Woo, J.H., Carmichael, G.R., 2003. Biomass burning in Asia: annual and seasonal estimates and atmospheric emissions. *Glob. Biogeochem. Cycles*. <http://dx.doi.org/10.1029/2003GB002040>.
- Szynkiewicz, A., Modelska, M., Jędrysek, M.O., Mastalerz, M., 2008. The effect of acid rain and altitude on concentration, $\delta^{34}\text{S}$, and $\delta^{18}\text{O}$ of sulfate in the water from Sudety Mountains, Poland. *Chem. Geol.* 249, 36–51.
- Tichomirowa, M., Heidel, C., 2012. Regional and temporal variability of the isotope composition (O, S) of atmospheric sulphate in the region of Freiberg, Germany, and consequences for dissolved sulphate in groundwater and river water. *Isot. Environ. Health Stud.* 48 (1), 118–143.
- Tsai, I.C., Chen, J.P., Lin, P.Y., Wang, W.C., Isaksen, I.S.A., 2010. Sulfur cycle and sulfate radiative forcing simulated from a coupled global climate–chemistry model. *Atmos. Chem. Phys.* 10, 3693–3709.
- Ullerstam, M., Vogt, R., Langer, S., Ljungstrom, E., 2002. The kinetics and mechanism of SO_2 oxidation by O_3 on mineral dust. *Phys. Chem. Chem. Phys.* 4, 4694–4699.
- Usher, C.R., Al-Hosney, H., Carlos-Cuellar, S., Grassian, V.H., 2002. A laboratory study of the heterogeneous uptake and oxidation of sulfur dioxide on mineral dust particles. *J. Geophys. Res. Atmos.* 107. <http://dx.doi.org/10.1029/2002JD002051>.
- Wadleigh, M.A., Schwarcz, H.P., Kramer, J.R., 1996. Isotopic evidence for the origin of sulphate in coastal rain. *Tellus B* 48B, 44–59.
- Wang, H., Han, G., 2011. Chemical composition of rainwater and anthropogenic influences in Chengdu, Southwest China. *Atmos. Res.* 99 (2), 190–196.
- Winterholler, B., Hopee, P., Huth, J., Foley, S., Andreae, M.O., 2008. Sulfur isotope analyses of individual aerosol particles in the urban aerosol at a central European site (Mainz, Germany). *Atmos. Chem. Phys. Discuss.* 8, 9347–9404.
- Xiao, H.W., Xiao, H.Y., Wang, Y.L., Tang, C.G., Liu, X.Y., 2010. Chemical characteristics of 9 d continuous precipitation in a typical polluted city: a case study of Guiyang. *Environ. Sci.* 31, 865–870 (in Chinese with English abstract).
- Xiao, H.W., Xiao, H.Y., Long, A.M., Wang, Y.L., 2011. Sulfur isotopic geochemical characteristics in precipitation at Guiyang. *Geochimica* 40, 559–565 (in Chinese with English abstract).
- Xiao, H.W., Xiao, H.Y., Long, A., Wang, Y.L., 2012. Who controls the monthly variations of NH_4^+ nitrogen isotope composition in precipitation? *Atmos. Environ.* 54, 201–206.
- Xiao, H.W., Xiao, H.Y., Long, A.M., Wang, Y.L., Liu, C.Q., 2013. Chemical composition and source apportionment of rainwater at Guiyang, SW China. *J. Atmos. Chem.* 70, 269–281.
- Xiao, H.W., Long, A.M., Xie, L.H., Xiao, H.Y., Liu, C.Q., 2014. Chemical characteristics of precipitation in South China Sea. *Environ. Sci.* 35, 475–480 (in Chinese with English abstract).
- Xiao, H., Liu, C., 2002. Sources of nitrogen and sulfur in wet deposition at Guiyang, southwest China. *Atmos. Environ.* 36 (33), 5121–5130.
- Xiao, H.Y., Liu, C.Q., 2004. Chemical characteristics of water-soluble components in TSP over Guiyang, SW China, 2003. *Atmos. Environ.* 38, 6297–6306.
- Xiao, H.Y., Tang, C.G., Xiao, H.W., Liu, X.Y., Liu, C.Q., 2009. Identifying the change in atmospheric sulfur sources in China using isotopic ratios in mosses. *J. Geophys. Res.* 114. <http://dx.doi.org/10.1029/2009JD012034>.
- Xu, Y.W., Carmichael, G.R., 1999. An assessment of sulfur deposition pathways in Asia. *Atmos. Environ.* 33, 3473–3486.
- Yang, F., Tan, J., Shi, Z.B., Cai, Y., He, K., Ma, Y., Duan, F., Okuda, T., Tanaka, S., Chen, G., 2012. Five-year record of atmospheric precipitation chemistry in urban Beijing, China. *Atmos. Chem. Phys.* 12, 2025–2035.
- Yang, Z., Kanda, K., Tsuruta, H., Minami, K., 1996. Measurement of biogenic sulfur gases emission from some Chinese and Japanese soil. *Atmos. Environ.* 30, 2399–2405.
- Zhao, D., Xiong, J., Xu, Y., Chan, W.H., 1988. Acid rain in southwestern China. *Atmos. Environ.* (1967) 22 (2), 349–358.
- Zhang, H.B., Hu, A.Q., Lu, C.Z., Zhang, G.X., 2002. Sulfur isotopic composition of acid deposition in South China Regions and its environmental significance. *China Environ. Sci.* 22 (2), 165–169 (in Chinese with English abstract).
- Zhang, M., Wang, S., Wu, F., Yuan, X., Zhang, Y., 2007. Chemical compositions of wet precipitation and anthropogenic influences at a developing urban site in southeastern China. *Atmos. Res.* 84 (4), 311–322.
- Zhang, W., Liu, C.Q., Li, X.D., Liu, T.Z., Zhang, L.L., 2010. Sulfur isotope ratios indicating sulfur cycling in slope soils of karst areas. *Environ. Sci.* 31, 415–422 (in Chinese with English abstract).
- Zhang, Y.M., Mitchell, M., Christ, M., Likens, G., Krouse, H.R., 1998. Stable sulfur isotopic biogeochemistry of the Hubbard Brook Experimental Forest, New Hampshire. *Biogeochemistry* 41, 259–275.
- Zimmermann, F., Matschullat, J., Brüggemann, E., Pleßow, K., Wienhaus, O., 2006. Temporal and elevation-related variability in precipitation chemistry from 1993 to 2002, Eastern Erzgebirge, Germany. *Water Air Soil Pollut.* 170 (1–4), 123–141.